

Received October 31, 2018, accepted November 8, 2018, date of publication November 19, 2018,
date of current version December 19, 2018.

Digital Object Identifier 10.1109/ACCESS.2018.2882128

Weighted Harvest-Then-Transmit: UAV-Enabled Wireless Powered Communication Networks

SUNGRYUNG CHO¹, KYUNGRAK LEE², BOOJOONG KANG³,
KWANGMIN KOO¹, AND INWHEE JOE⁴

¹Department of Computer and Software, Hanyang University, Seoul 04763, South Korea

²Unmanned Vehicle Systems Research Group, Electronics and Telecommunications Research Institute, Daejeon 34129, South Korea

³Centre for Secure Information Technology, Queen's University Belfast, Belfast BT3 9DT, U.K.

⁴Department of Computer Science and Engineering, Hanyang University, Seoul 04763, South Korea

Corresponding author: Inwhee Joe (iwjoe@hanyang.ac.kr)

This work was supported by the National Research Foundation of Korea (NRF) funded by the Korea Government (Ministry of Science, ICT & Future Planning) under Grant 2016R1A2B4013118.

ABSTRACT This paper proposes an unmanned aerial vehicle (UAV)-enabled wireless-powered communication network (WPCN), which consists of a hybrid access point (H-AP), a UAV, and nodes. The H-AP broadcasts energy to all nodes, and the nodes harvest and use the energy for information transmission. However, far-apart nodes from the H-AP hardly harvest the energy and they require more energy for the same throughput as near-apart nodes due to distance-dependent signal attenuation, which is called the doubly near-far problem. To overcome the doubly near-far problem, we propose a weighted harvest-then-transmit protocol. In the proposed protocol, we consider that the channel power gain changes according to the location of nodes, whereas it has remained constant in most conventional WPCNs. The UAV acts as a mobile H-AP, where the UAV performs weighted energy transfer and receives information to/from all encountering far-apart nodes with the better channel power gain. For the UAV, we consider the flight path optimization by implementing a regression algorithm in terms of energy efficiency. Under these considerations, we aim to maximize the sum-throughput of all nodes based on the weighted harvest-then-transmit protocol, by using convex optimization techniques. The optimal time allocation is investigated for far-apart nodes and near-apart nodes sequentially, to solve the doubly near-far problem. Simulation results show that the proposed UAV-enabled WPCN outperforms the conventional WPCN with a fixed H-AP in terms of the sum-throughput maximization.

INDEX TERMS Convex optimization, doubly-near-far problem, sum-throughput maximization, unmanned aerial vehicle, UAV-enabled wireless-powered communication networks, weighted harvest-then-transmit, wireless-powered communication networks.

I. INTRODUCTION

A. MOTIVATIONS AND RELATED WORKS

Energy management at individual nodes is one of the most challenging issues in wireless networks. Energy management strategies can be different depending on what energy source is being used. Traditional energy sources (e.g., batteries) for wireless devices are physically attached to the devices and need to be replaced or recharged periodically. This will limit the operation time of wireless devices and affect the performance of wireless networks.

Recently, an energy harvesting technique that utilizes radio frequency (RF) signals has emerged as an alternative method to recharge nodes in wireless networks [1], [2]. Ambient radio signals controlled by a transmitter enable both wireless

energy transfer (WET) and wireless information transfer (WIT) [3], [4]. The feasibility of WET and WIT has been demonstrated in the recent experimental works [5]–[7] and the recently proposed models of wireless-powered communication networks (WPCNs) support both WET and WIT using radio signals [8]–[12]. The initial model of WPCN [13] is composed of a hybrid-access point (H-AP) and multiple end nodes. In order to avoid the interference between energy and information signals, Ju and Zhang [13] proposed a harvest-then-transmit protocol based on time division multiple access (TDMA). For better performance of WPCN, full-duplex models are presented in [14]–[17], where the H-AP broadcasts wireless energy to the nodes in the downlink (DL) and the nodes transmit their information in the uplink (UL)

at the same time. In [18], we also have studied a full-duplex model for a mesh-topology network considering node-to-node communication. For a large-scale network, a carrier-sense multiple access (CSMA) based model is also proposed in [19]. However, these prior researches have hardly considered the distance-dependent signal attenuation (e.g., channel power gain) that might lead to the *doubly-near-far* problem [4], [20]. Far-apart nodes from the H-AP harvest less energy compared to near-apart nodes, and the far-apart nodes require more energy for the same throughput of the near-apart nodes.

Several WPCN models were further proposed to reduce the influence of the distance-dependent signal attenuation. Ju and Zhang [13] considered an additional constraint that guarantees the equal throughput of all nodes regardless of the channel power gain to the H-AP. In [21], a dedicated relay node is proposed to help far-apart nodes to transmit information, where the relay node amplifies the received signal and forwards it to the destination. Bi and Zhang [22] proposed to divide the H-AP into two dedicated access points: the energy access point for WET and the information access point for WIT. They also optimized the location of the two access points to minimize the overall cost. However, most of the existing studies still assumed that the channel power gain in DL and UL remains constant, despite the fact that the channel power gain changes according to the distance between network units (e.g., access point and nodes) in DL WET and UL WIT.

Meanwhile, a unmanned aerial vehicle (UAV)-enabled network systems have recently come into the spotlight due to their advantages in strong line-of-sight (LoS) to nodes, controllable mobility, and flexible wireless connectivity without infrastructure [25]–[27]. In [25], a high-mobility UAV is deployed to assist the information transmission between ground sources and destinations, in order to maximize the spectrum efficiency and energy efficiency. Besides, in [26], a UAV is utilized as a mobile data sink for ground sensor nodes in wireless sensor networks. In addition, Zeng *et al.* [28] provide various applications of UAV integrated into the cellular network. Inspired by the advantage of UAV-assisted wireless communications, UAV-enabled wireless power transfer (WPT) has been proposed in [28] and [29]. Specifically, in [29], a UAV is considered as a mobile energy transmitter broadcasting wireless energy to charge the nodes on the ground while hovering over the nodes. Furthermore, in [30], a UAV is integrated into WPCN, where the UAV performs WET in DL to charge the nodes, and the nodes use the harvested energy to send information to the UAV in UL. The authors try to maximize the uplink minimum throughput among all nodes over a given UAV's flight time. However, the channel power gain is still assumed to be constant in most prior researches.

B. GOALS

In this paper, we propose a UAV-enabled WPCN that adopts a UAV to overcome the *doubly-near-far* problem.

The proposed UAV-enabled WPCN consists of a H-AP, a UAV, and nodes. The H-AP transmits energy to nodes and receives information from nodes. We divide nodes into two types according to the channel power gain between the H-AP and each node. The first one is a high gain node (HGN), where the channel power gain between the H-AP and the node is higher than a given threshold. It is worth noting that the threshold depends on the system of interest. The other type is a low gain node (LGN), where the channel power gain between the H-AP and a node is lower than the threshold. This means that the node hardly harvests energy from the H-AP, i.e., LGNs suffer from the *doubly-near-far* problem. We assume that LGNs are located far from the H-AP compared to HGNs since the channel power gain largely depends on the communication distance.

The UAV acts as a mobile H-AP in the proposed UAV-enabled WPCN. For the UAV-enabled WPCN, we propose a *weighted harvest-then-transmit* protocol (WHT). The flight of the UAV in the proposed WHT can be separated into two phases: the forward flight phase and the return flight phase. In the forward flight phase, the UAV starts its flight at the H-AP and flies toward the farthest node from the H-AP within the communication range of the H-AP. During the forward flight phase, the UAV performs the weighted DL WET to all encountering LGNs, where the amount of transmitted energy to each LGN is inversely proportional to the channel power gain between the H-AP and each LGN. It is worth noting that the UAV does not perform the weighted DL WET to HGNs since the UAV is employed to solve the *doubly-near-far* problem. After arriving at the farthest node from the H-AP, the UAV gets into the return flight phase, where the UAV returns to the H-AP following the reverse of the forward flight path. During the return flight phase, the UAV receives information from the encountering LGNs. The LGNs transmit their information to the UAV when the UAV is close enough to reduce the energy loss with the better channel power gain between the UAV and LGNs, while the HGNs transmit their information directly to the H-AP.

We also propose channel-weighted path (CWP) planning, based on the regression algorithm [31], for the optimal flight path of the UAV in terms of energy efficiency. An initial flight path is computed with the hypothesis of CWP and then trained by optimizing the loss function [32] of the regression. The loss function considers the channel power gain between the UAV and LGNs, and also the distance of each LGN from the initial flight path.

The main contributions of this paper are summarized as follows:

- We propose a new WPCN model to solve the *doubly-near-far* problem. Our UAV-enabled WPCN has two H-APs: a conventional fixed H-AP and a new mobile H-AP employing a UAV.
- We propose a *weighted harvest – then – transmit* protocol for the proposed UAV-enabled WPCN. The UAV adopting WHT performs the weighted DL WET to LGNs in the forward flight phase, and receive

information from the LGNs in the return flight phase. Accordingly, the LGNs can harvest energy from the UAV with the minimum energy loss caused by energy signal attenuation, and transmit information to the UAV energy-efficiently. Consequently, the *doubly-near-far* problem at the LGNs can be alleviated.

- We propose the channel-weighted path planning to optimize the flight path of the UAV in terms of energy efficiency. The initial flight path is trained according to the channel power gain and the distance between the initial flight path and LGNs. Thus, the flight path of the UAV is optimized to reduce the flight time and energy.
- For investigating the performance of the proposed WHT protocol in the UAV-enabled WPCN, we study the sum-throughput maximization problems using convex optimization techniques.

The rest of this paper is organized as follows. Section 2 proposes the UAV-enabled WPCN model and the proposed WHT protocol. Section 3 presents the sum-throughput maximization based on the proposed WHT protocol in the UAV-enabled WPCN. Section 4 analyzes the influence of the flight time in terms of the sum-throughput maximization. Section 5 shows numerical results. Finally, Section 6 concludes the paper and debates future work.

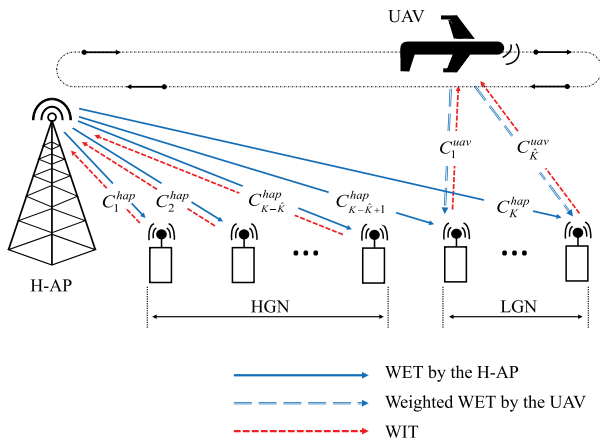


FIGURE 1. System model: UAV-enabled wireless powered communication network.

II. SYSTEM MODEL

In this section, we propose the proposed UAV-enabled WPCN and the *weighted harvest – then – transmit* protocol. As shown in Fig. 1, the UAV-enabled WPCN consists of a single H-AP, a UAV, and node $i, \forall i \in \{1, 2, \dots, K\}$, where K is a positive integer. We divide nodes into two types, i.e., HGN and LGN, according to the channel power gain between the H-AP and each node. We assume that LGNs suffer from the *doubly-near-far* problem, since their channel power gain to the H-AP is lower than the required threshold. Note that near-apart node can be a LGN when it has lower channel power gain than the threshold due to poor network environment such as the shadowing. The number of LGNs is

denoted by \hat{K} , thus the number of HGN is $K - \hat{K}$. We assume that the H-AP and the UAV equip single antenna for the DL WET and receiving information from nodes. Note that the UAV employs directional beamforming to construct a focused energy beam to individual LGN [2], [33]. It is assumed that the UAV hovers when transmitting energy and receiving information, hence we also assume that there is no Doppler effect while transmitting energy and receiving information. All nodes are also assumed to have a single antenna for harvesting energy and the UL WIT. Therefore, they cannot harvest energy and transmit information at the same time. It is worth noting that all network units, i.e., the H-AP, the UAV and nodes, operate over a same frequency band. In addition, all nodes in the proposed network are assumed to have no other energy source except the energy transmitted by the H-AP and the UAV.

We assume that both the DL and UL channels between the H-AP and HGNs are complex random variables denoted by $\tilde{C}_i^{hap,dl}$ and $\tilde{C}_i^{hap,ul}, \forall i \in \{1, 2, \dots, K\}$, respectively. Also, we assume that both the DL and UL channels are quasi-static flat-fading. Thus, the DL channel power gain and corresponding reversed UL channel power gain between the H-AP and node $i, \forall i \in \{1, 2, \dots, K\}$, are denoted by $C_i^{hap,dl} = |\tilde{C}_i^{hap,dl}|^2$ and $C_i^{hap,ul} = |\tilde{C}_i^{hap,ul}|^2$, respectively. Then, $C_i^{hap,dl}$ and $C_i^{hap,ul}$ can be expressed as [23], [24]

$$C_i^{hap,dl} = G_{hap}^{tx} G_i^{rx} \left(\frac{v/f_c}{4\pi d_i^{hap}} \right)^2, \quad \forall i \in \{1, 2, \dots, K\}, \quad (1)$$

$$C_i^{hap,ul} = G_{hap}^{rx} G_i^{tx} \left(\frac{v/f_c}{4\pi d_i^{hap}} \right)^2, \quad \forall i \in \{1, 2, \dots, K\}, \quad (2)$$

where G_{hap}^{tx} and G_{hap}^{rx} are the antenna gains of the H-AP while transmitting and receiving, respectively. Also, G_i^{tx} and G_i^{rx} are the antenna gains of node $i, \forall i \in \{1, 2, \dots, K\}$, while transmitting and receiving, respectively. v indicates the speed of light and f_c indicates a carrier frequency, respectively. d_i^{hap} indicates the distance between the H-AP and node $i, \forall i \in \{1, 2, \dots, K\}$.

Moreover, we assume that both the DL and UL channels between the UAV and LGNs are complex random variables denoted by $\tilde{C}_i^{uav,dl}$ and $\tilde{C}_i^{uav,ul}, \forall i \in \{1, 2, \dots, \hat{K}\}$, respectively, which follows the same assumption as $\tilde{C}_i^{hap,dl}$ and $\tilde{C}_i^{hap,ul}$. Then, the DL channel power gain and corresponding reversed UL channel power gain between the UAV to LGN $i, \forall i \in \{1, 2, \dots, \hat{K}\}$, are denoted by $C_i^{uav,dl} = |\tilde{C}_i^{uav,dl}|^2$ and $C_i^{uav,ul} = |\tilde{C}_i^{uav,ul}|^2$, respectively. Then, $C_i^{uav,dl}$ and $C_i^{uav,ul}$ can be expressed as [23], [24]

$$C_i^{uav,dl} = G_{uav}^{tx} G_i^{rx,lg} \left(\frac{v/f_c}{4\pi d_i^{uav}} \right)^2, \quad \forall i \in \{1, 2, \dots, \hat{K}\}, \quad (3)$$

$$C_i^{uav,ul} = G_{uav}^{rx} G_i^{tx,lg} \left(\frac{v/f_c}{4\pi d_i^{uav}} \right)^2, \quad \forall i \in \{1, 2, \dots, \hat{K}\}, \quad (4)$$

where G_{uav}^{tx} and G_{uav}^{rx} are the antenna gains of the UAV while transmitting and receiving, respectively. Also, $G_i^{rx,lg}$

and G_i^{Lgn} are the antenna gains of LGN $i, \forall i \in \{1, 2, \dots, \hat{K}\}$, respectively. d_i^{uav} indicates the distance between the UAV and LGN $i, \forall i \in \{1, 2, \dots, \hat{K}\}$. For the purpose of exposition, it is assumed that the DL and UL channel power gain at the H-AP and the UAV are equal, i.e., $C_i^{hap,dl} = C_i^{hap,ul}$ and $C_i^{uav,dl} = C_i^{uav,ul}$, respectively, in the sequel. Therefore, the channel power gain of DL and UL at the H-AP is denoted by C_i^{hap} and at the UAV is denoted by C_i^{uav} , respectively. During a block time, denoted by T , C_i^{hap} remains constant, but can possibly vary from one block to another, depending on the system of interest. It is also assumed that the H-AP perfectly knows $C_i^{hap}, \forall i \in \{1, 2, \dots, K\}$.

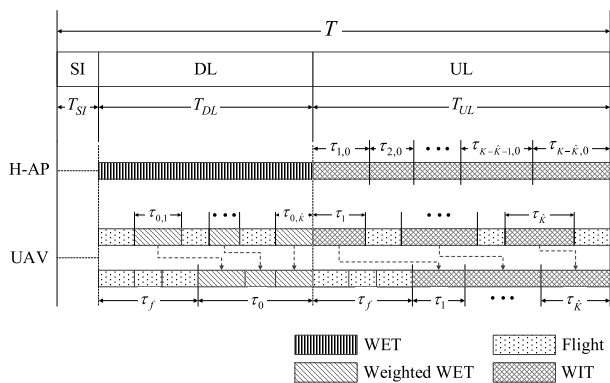


FIGURE 2. The weighted harvest-then-transmit protocol in UAV-enabled WPCN.

A. BLOCK STRUCTURE IN THE WEIGHTED HARVEST-THEN-TRANSMIT PROTOCOL

The UAV-enabled WPCN adopts the proposed WHT protocol to overcome the *doubly-near-far* problem as shown in Fig. 2. The block in the WHT protocol consists of state information (SI) transmission period, DL period, and UL period in a block time, where each duration time of these periods is denoted by T_{SI}, T_{DL} , and T_{UL} , respectively. Therefore, we have

$$T = T_{SI} + T_{DL} + T_{UL}. \quad (5)$$

For convenience, a block time is normalized as $T = 1$; hence, both the term of energy and power can be interchangeable.

The SI period contains the energy beacon period, SI transfer period, and command transfer period [19]. The H-AP broadcasts energy to all nodes during the energy beacon period, and the nodes harvest the energy. During the SI transfer period, the nodes report their own SI using the harvested energy. Note that the harvested energy during the energy beacon period is only used and sufficient for the SI transmission. In addition, the excess energy after SI transmission is negligible since the overall energy is quite low. We assume that the SI includes a longitude and a latitude of nodes from Global Positioning System (GPS). During the command transfer period, the H-AP classifies nodes into HGN and LGN, and decides the flight path of the UAV based on the received SI. Also, the optimal time of the weighted DL WET

for each LGN is calculated. Then, the H-AP transmits the command to the UAV and all nodes, in order to inform the decision information. Therefore, we have

$$T_{SI} = \tau_{eb} + \tau_{sit} + \tau_{cmd}, \quad (6)$$

where τ_{eb} , τ_{sit} , and τ_{cmd} denote the duration time of energy beacon period, SI transfer period, and command transfer period, respectively. We assume that τ_{eb} , τ_{sit} , and τ_{cmd} are negligible, hence T_{SI} is zero for convenience, as [24] and [35].

During the DL period, the H-AP performs the DL WET to all nodes, i.e., HGNs and LGNs. Meanwhile, the UAV performs the weighted DL WET only to LGNs to overcome the *doubly-near-far* problem. Then, T_{DL} can be expressed as

$$T_{DL} = \tau_f + \tau_0 \quad (7)$$

$$= \frac{d_f}{v_{uav}} + \tau_0, \quad (8)$$

where τ_f , d_f , and v_{uav} denote the flight time in the forward flight phase, distance of the flight path, and the speed of the UAV, respectively. Note that for convenience, we assume that the UAV flies at constant speed. We also assume that the return flight path of the UAV is same as the reverse of the forward flight path. Therefore, the total flight distance is $2d_f$ in one block time. τ_0 denotes the total weighted DL WET time of the UAV in a block time, which can be expressed as

$$\tau_0 = \sum_{i=1}^{\hat{K}} \tau_{0,i}, \quad \forall i \in \{1, 2, \dots, \hat{K}\}, \quad (9)$$

where $\tau_{0,i}$ denotes the weighted DL WET time for LGN $i, \forall i \in \{1, 2, \dots, \hat{K}\}$.

During the UL period, the LGN $i, \forall i \in \{1, 2, \dots, \hat{K}\}$, powered by the UAV, transmits information to the UAV in the return flight phase. Then, T_{UL} can be expressed as

$$T_{UL} = \tau_f + \sum_{i=1}^{\hat{K}} \tau_i, \quad \forall i \in \{1, 2, \dots, \hat{K}\}. \quad (10)$$

On the other hand, HGNs also perform the UL WIT directly to the H-AP in the return phase. Therefore, T_{UL} can be also expressed as

$$T_{UL} = \sum_{i=1}^{K-\hat{K}} \tau_{i,0}, \quad \forall i \in \{1, 2, \dots, K-\hat{K}\}. \quad (11)$$

where $\tau_{i,0}$ denotes the UL WIT time from HGNs to the H-AP. Since $\tau_0, \tau_1, \dots, \tau_{\hat{K}}$ represent the time allocated to the UAV for the weighted DL WET and to LGNs for the UL WIT, respectively, we have

$$\sum_{i=0}^{\hat{K}} \tau_i \leq 1 - 2\tau_f, \quad \forall i \in \{0, 1, \dots, \hat{K}\}. \quad (12)$$

B. THE WIRELESS ENERGY TRANSFER IN THE WEIGHTED HARVEST-THEN-TRANSMIT PROTOCOL

In the DL period, the H-AP broadcasts energy to all nodes and the harvested energy at node i , $\forall i \in \{1, 2, \dots, K\}$, denoted by E_i^{hap} , can be expressed as

$$E_i^{hap} = \xi_i^{hap} C_i^{hap} P_H T_{DL} \tag{13}$$

$$= \xi_i^{hap} C_i^{hap} P_H \left(\frac{d_f}{v_{uav}} + \tau_0 \right), \quad \forall i \in \{1, 2, \dots, K\}, \tag{14}$$

where $0 \leq \xi_i^{hap} \leq 1$ indicates the energy harvesting efficiency at node i , $\forall i \in \{1, 2, \dots, K\}$. P_H is the transmit power at the H-AP, where the H-AP has a stable energy supply to provide power in wireless. Therefore, P_H is assumed to be sufficient to ignore the received noise at nodes.

For the LGNs, the UAV transmits energy to LGN i , $\forall i \in \{1, 2, \dots, \hat{K}\}$, when the UAV is close enough to reduce the energy loss with the better channel power gain, C_i^{uav} . Note that we assume that LGNs are far-apart from the H-AP as we consider the doubly-near-far problem. Then, the harvested energy at LGNs, denoted by E_i^{uav} , can be expressed as

$$E_i^{uav} = \xi_i^{uav} C_i^{uav} P_U \tau_{0,i}, \quad \forall i \in \{1, 2, \dots, \hat{K}\}, \tag{15}$$

where $0 \leq \xi_i^{uav} \leq 1$ indicates the energy harvesting efficiency at LGN i , $\forall i \in \{1, 2, \dots, \hat{K}\}$. P_U is the transmit power at the UAV. We assume that the UAV performs the weighted DL WET to node i , $\forall i \in \{1, 2, \dots, \hat{K}\}$, as hovering above the node i and the time of the weighted DL WET to the node i is inversely proportional to the channel power gain between the H-AP and each LGN. Therefore, the time of the weighted DL for each node is denoted by $\tau_{0,i}$, which is given by

$$\tau_{0,i} = \frac{\tau_0}{C_i^{hap} \sum_{j=1}^{\hat{K}} \frac{1}{C_j^{hap}}}, \quad \forall i \in \{1, 2, \dots, \hat{K}\}. \tag{16}$$

For the energy causality of the UAV, we have

$$Q_{uav} \leq Q_{flight} + Q_{wdl} + Q_{hv}, \tag{17}$$

where Q_{flight} , Q_{wdl} and Q_{hv} denote the total amount of the energy for the flight, for the weighted DL WET, and for the hovering to perform the weighted DL WET and the UL WIT in a block time, respectively. Q_{uav} denotes the amount of total energy available in the UAV. We assume that Q_{uav} is fully charged when the UAV starts the flight at the H-AP and the UAV has no other energy consumption except Q_{flight} , Q_{wdl} , and Q_{hv} . Hence, it is assumed that $Q_{uav} = Q_{flight} + Q_{wdl} + Q_{hv}$ in the sequel, i.e., all the energy of the UAV, Q_{uav} , is used in a block time.

Consequently, all nodes in the UAV-enabled WPCN harvest energy from the H-AP and the UAV, i.e., HGNs harvest energy transmitted by the H-AP only, while LGNs harvested energy transmitted by the H-AP and the UAV. The total harvested energy at nodes is denoted by E_i^{total} , which can be expressed as

$$E_i^{total} = E_i^{hap} + \rho_i E_i^{uav} \tag{18}$$

$$= \xi_i^{hap} C_i^{hap} P_H \left(\frac{d_f}{v_{uav}} \right) + \xi_i^{hap} C_i^{hap} P_H \tau_0 + \rho_i \xi_i^{uav} C_i^{uav} P_U \frac{\tau_0}{C_i^{hap} \sum_{j=1}^{\hat{K}} \frac{1}{C_j^{hap}}} \tag{19}$$

$$= \xi_i^{hap} C_i^{hap} P_H \left(\frac{d_f}{v_{uav}} \right) + \xi_i^{hap} C_i^{hap} P_H \tau_0 + \rho_i \xi_i^{uav} C_i^{uav} \frac{Q_{wdl}}{C_i^{hap} \sum_{j=1}^{\hat{K}} \frac{1}{C_j^{hap}}}, \tag{20}$$

$\forall i \in \{1, 2, \dots, K\}$

where ρ_i is the choice indicator that is 1 if node i is classified to LGN due to low channel power gain, or is zero otherwise. We change the variable as $P_U \tau_0 = Q_{wdl}$ from (9) and (17). For convenience, it is assumed that $\xi_i^{hap} = \xi_i^{uav} = \xi_i$ in the sequel of this paper.

C. THE WIRELESS INFORMATION TRANSFER IN THE WEIGHTED HARVEST-THEN-TRANSMIT PROTOCOL

In the UL period, all nodes perform the UL WIT using their total harvested energy in (18). The LGN i , $\forall i \in \{1, 2, \dots, \hat{K}\}$, performs its UL WIT to the UAV when the UAV is hovering above the LGN i , in order to reduce the transmission power. Note that C_i^{uav} is an optimal constant value during the UL WIT, since the UAV is close enough to each LGN i . Also, the HGN i , $\forall i \in \{1, 2, \dots, K - \hat{K}\}$, performs its UL WIT to the H-AP.

For the throughput maximization, nodes consume all harvested energy for their UL WIT. We denote x_i as the complex baseband signal transmitted by node i , $\forall i \in \{1, 2, \dots, K\}$, which is Gaussian inputs, i.e., $x_i \sim \mathcal{CN}(0, P_i^{hap})$ and $x_i \sim \mathcal{CN}(0, P_i^{uav})$, where P_i^{hap} and P_i^{uav} denote the average transmit power at nodes to the H-AP and the UAV, respectively. Then, P_i^{hap} during the UL period at HGN i , $\forall i \in \{1, 2, \dots, K - \hat{K}\}$, can be expressed as

$$P_i^{hap} = \frac{\zeta_i^{hap} E_i^{total}}{\tau_{i,0}}, \quad \forall i \in \{1, 2, \dots, K - \hat{K}\}, \tag{21}$$

where $0 \leq \zeta_i^{hap} \leq 1$ denotes the portion of the total harvested energy used for the UL WIT at HGNs in steady state. We assume $\zeta_i = 1$, $\forall i \in \{1, 2, \dots, K - \hat{K}\}$, i.e., all the harvested energy at HGN i , $\forall i \in \{1, 2, \dots, K - \hat{K}\}$, is consumed for its UL WIT. On the other hand, P_i^{uav} can be expressed as

$$P_i^{uav} = \frac{\zeta_i^{uav} E_i^{total}}{\tau_i}, \quad \forall i \in \{1, 2, \dots, \hat{K}\}, \tag{22}$$

where $0 \leq \zeta_i^{uav} \leq 1$ denotes the portion of the total harvested energy used for the UL WIT at LGNs in steady state, which follows the same assumption as ζ_i^{hap} .

Then, from (18)-(22), the achievable UL throughput of LGN i , $\forall i \in \{1, 2, \dots, \hat{K}\}$, can be expressed as

$$R_i^{uav} = \tau_i \ln \left(1 + \frac{C_i^{uav} P_i^{uav}}{\Gamma \sigma^2} \right) \tag{23}$$

$$\begin{aligned}
&= \tau_i \ln \left(1 + \frac{C_i^{uav} E_i^{total}}{\Gamma \sigma^2 \tau_i} \right) \\
&= \tau_i \ln \left(1 + \varepsilon_i \frac{1}{\tau_i} + \hat{\varepsilon}_i \frac{\tau_0}{\tau_i} \right), \quad \forall i \in \{1, 2, \dots, \hat{K}\},
\end{aligned} \tag{24}$$

$$\tag{25}$$

where ε_i and $\hat{\varepsilon}_i$ are denoted by $\varepsilon_i = \frac{\xi_i C_i^{uav}}{\Gamma \sigma^2} \left(\frac{C_i^{hap} P_H d_f}{v_{uav}} + \frac{C_i^{uav} Q_{wdl}}{C_i^{hap} \sum_{j=1}^{\hat{K}} \frac{1}{C_j^{hap}}} \right)$ and $\hat{\varepsilon}_i = \frac{\xi_i C_i^{uav} C_i^{hap} P_H}{\Gamma \sigma^2}$, respectively. Γ denotes the signal-to-noise ratio gap from the additive white Gaussian noise channel capacity as a modulation and coding scheme used [19]. σ^2 represents the noise power at the UAV.

In addition, the achievable UL throughput of HGN i , $\forall i \in \{1, 2, \dots, K - \hat{K}\}$, from (18)-(22), can be expressed as

$$R_i^{hap} = \tau_{i,0} \ln \left(1 + \frac{C_i^{hap} P_i^{hap}}{\Gamma \hat{\sigma}^2} \right) \tag{26}$$

$$= \tau_{i,0} \ln \left(1 + \frac{C_i^{hap} E_i^{total}}{\Gamma \hat{\sigma}^2 \tau_{i,0}} \right) \tag{27}$$

$$= \tau_{i,0} \ln \left(1 + \bar{\varepsilon}_i \frac{1}{\tau_{i,0}} \right), \quad \forall i \in \{1, 2, \dots, K - \hat{K}\}, \tag{28}$$

where $\bar{\varepsilon}_i$ is denoted by $\bar{\varepsilon}_i = \frac{\xi_i P_H (C_i^{hap})^2}{\Gamma \hat{\sigma}^2} \left(\frac{d_f}{v_{uav}} + \tau_0 \right)$ and $\hat{\sigma}^2$ denotes the noise power at the H-AP.

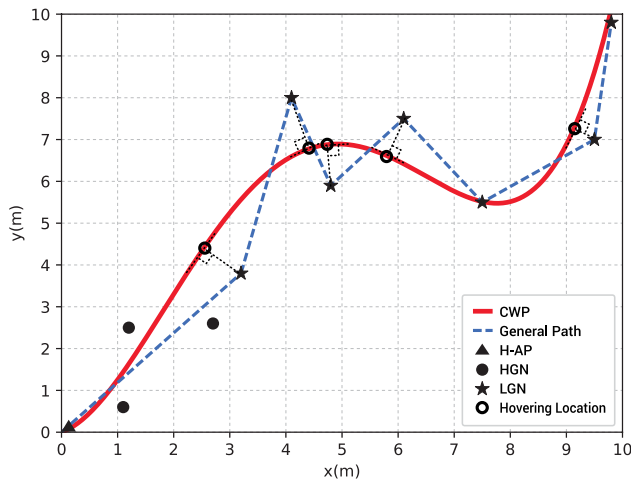


FIGURE 3. An example: the channel-weighted path planning.

D. THE CHANNEL-WEIGHTED PATH PLANNING FOR THE WEIGHTED HARVEST-THEN-TRANSMIT PROTOCOL

In this subsection, we describe the CWP planning to optimize the flight path of the UAV in terms of energy efficiency, as shown in Fig. 3. The UAV flies to LGNs and performs the weighted DL WET, and returns to the H-AP following the reverse of the forward flight path while receiving information from LGNs. The CWP planning is based on regression algorithm [31] that trains the hypothesis by optimizing the loss

function [32]. Note that the hovering location for the DL and UL is assumed to be shortest distance calculated by the CWP as shown in Fig. 3.

The flight path, denoted by $H(\alpha)$, is calculated as the hypothesis, which can be expressed as

$$H(\alpha) = \sum_{i=0}^l \theta_i \alpha^i, \tag{29}$$

where α denotes a longitude on the flight path and θ_i denotes the coefficient of α^i . Note that l is the maximum power of $H(\alpha)$, which is depending on the system of interest.

The flight path is trained by the channel power gain and the distance between the initial flight path and LGNs. For the training, we consider the loss function, denoted by $L(x)$, which is given by

$$L(\beta_i) = \sum_{i=1}^{\hat{K}} \frac{1}{\hat{K}} \omega_i (\kappa_i - H(\beta_i))^2, \tag{30}$$

where β_i and κ_i denote the longitude and the latitude of LGN i , $\forall i \in \{1, 2, \dots, \hat{K}\}$. Also, ω_i indicates the weight of LGN i , $\forall i \in \{1, 2, \dots, \hat{K}\}$, depending on the channel power gain to the UAV, C_i^{uav} , and the distance between the initial flight path and LGNs. Note that ω_i is initialized by 1 at the first, and increases as the distance increases, but as C_i^{uav} decreases. In this manner, a minimum value of $L(\beta_i)$ and optimal θ_i can be derived, using Gradient Descent method [34]. The optimal θ_i updates $H(w)$ to find the optimal flight path. To summarize, the CWP planning algorithm is described in Table 1.

TABLE 1. CWP planning algorithm.

1. Initialize GPS data of LGN i , $\forall i \in \{1, 2, \dots, \hat{K}\}$.
2. Initialize $H(\alpha)$ with random θ_i and $L(x_i)$ with $\omega_i = 1$.
3. **repeat**.
4. Compute the gradient using Gradient decent method, i.e., $\frac{\partial L(\beta_i)}{\partial \theta_i}$.
5. Update θ_i to $H(\alpha)$.

$$\theta_i = \theta_i - \frac{\partial L(\beta_i)}{\partial \theta_i}$$
6. Update ω_i to $L(\beta_i)$.
 If ω_i increases as the distance increases, but as C_i^{uav} decreases.
7. **until** Find $H(\alpha)$ with optimal θ_i .

III. PROBLEM FORMULATION FOR THE WEIGHTED HARVEST-THEN-TRANSMIT PROTOCOL

In the proposed UAV-enabled WPCN, nodes can perform their UL WIT to the H-AP or the UAV, i.e., HGNs transmit their information to the H-AP, whereas LGNs transmit information to the UAV when the UAV is close to them to reduce the transmission power. Therefore, the sum-throughput of all nodes can be expressed as

$$R_{sum} = \sum_{i=1}^{\hat{K}} R_i^{uav} + \sum_{j=1}^{K-\hat{K}} R_j^{hap}. \tag{31}$$

Consequently, from (23) and (26), the sum-throughput can be equivalently expressed as

$$R_{sum} = \sum_{i=1}^{\hat{K}} \tau_i \ln \left(1 + \varepsilon_i \frac{1}{\tau_i} + \hat{\varepsilon}_i \frac{\tau_0}{\tau_i} \right) + \sum_{j=1}^{K-\hat{K}} \tau_{j,0} \ln \left(1 + \bar{\varepsilon}_j \frac{1}{\tau_{j,0}} \right). \quad (32)$$

To maximize the sum-throughput from (32), the optimal time allocation is firstly investigated for LGNs, as we consider the *doubly-near-far* problem. The sum-throughput of LGNs can be expressed as the following problem:

$$(P1): \quad \max_{\boldsymbol{\tau}} \sum_{i=1}^{\hat{K}} R_i^{uav}(\tau_i) \quad (33)$$

$$\text{s.t.} \quad \sum_{i=0}^{\hat{K}} \tau_i \leq 1 - 2\tau_f \quad (34)$$

$$\tau_i \geq 0, \quad \forall i \in \{0, 1, \dots, \hat{K}\} \quad (35)$$

$$Q_{uav} \leq Q_{flight} + Q_{wdl} + Q_{hv} \quad (36)$$

$$v_{uav} \geq 0. \quad (37)$$

To solve (P1) by convex optimization techniques, the objective of (P1) should be concave function and all the constraints of (P1) are affine. Thus, we firstly express the following two lemmas.

Lemma 4.1: The throughput function of LGN i , $\forall i \in \{1, 2, \dots, \hat{K}\}$, given by $R_i^{uav}(\tau_i)$, is a concave function of the nonnegative vector $\boldsymbol{\tau} = [\tau_0, \tau_1, \dots, \tau_{\hat{K}}]^T$.

Proof: Please refer to Appendix A.

Lemma 4.2: The optimal time allocation $\boldsymbol{\tau}^*$ of (P1) has to satisfy the constraint in (34) with equality, i.e., $\sum_{i=0}^{\hat{K}} \tau_i^* = 1 - 2\tau_f$.

Proof: Please refer to Appendix B.

According to [36], a nonnegative weighted summation of concave functions is concave. From Lemma 4.1 that the objective function of (P1) is a concave function of $\boldsymbol{\tau}$, where $R_i^{uav}(\tau_i)$ is concave function. In addition, in (P1), all the constraints are affine from Lemma 4.2. Hence, (P1) is a convex optimization problem clearly, which can be solved by using convex optimization techniques. Thus, we consider its Lagrangian duality, given by

$$\mathcal{L}(\boldsymbol{\tau}, \lambda) = \sum_{i=1}^{\hat{K}} R_i^{uav}(\tau_i) - \lambda \left(\sum_{i=0}^{\hat{K}} \tau_i + 2\tau_f - 1 \right), \quad (38)$$

where λ is the non-negative Lagrangian dual variable related to constraint given in (34). Thus, the dual function of (P1) can be expressed as

$$\mathcal{G}(\lambda) = \max_{\boldsymbol{\tau} \in \mathcal{D}} \mathcal{L}(\boldsymbol{\tau}, \lambda), \quad (39)$$

where \mathcal{D} is the feasible set of $\boldsymbol{\tau}$ specified by the constraints (34) and (35). We obtain the optimal time allocation solution of (P1) as the following proposition.

Proposition 4.1: The optimal time allocation of (P1) is

$$\tau_0^* = \frac{z^*(1 - \tau_f) - 1 + 2\tau_f - C \frac{\varepsilon_{\hat{K}}}{\varepsilon_{\hat{K}}}}{C + z^* - 1}, \quad (40)$$

$$\tau_i^* = \frac{\hat{\varepsilon}_i}{C} \left(\frac{C(1 - \frac{\varepsilon_{\hat{K}}}{\varepsilon_{\hat{K}}}) - z^* + 4\tau_f}{C + z^* - 1} - 2\tau_f \right), \quad \forall i \in \{1, 2, \dots, \hat{K}\}, \quad (41)$$

where $C \triangleq \sum_{i=1}^{\hat{K}} \hat{\varepsilon}_i > 0$. $z^* > 1$ is the corresponding solution of $f(z) = C$ where $f(z) \triangleq z \ln z - z + 1$.

Proof: Please refer to Appendix C.

Given τ_0^* and τ_i^* , $\forall i \in \{1, 2, \dots, \hat{K}\}$, the sum-throughput of HGNs can be expressed as the following problem:

$$(P2): \quad \max_{\boldsymbol{\tau}} \sum_{j=1}^{K-\hat{K}} R_j^{hap}(\tau_{j,0}) \quad (42)$$

$$\text{s.t.} \quad \sum_{i=1}^{K-\hat{K}} \tau_{i,0} \leq 1 - \tau_f - \tau_0^* \quad (43)$$

$$\tau_{i,0} \geq 0, \quad \forall i \in \{0, 1, \dots, K - \hat{K}\}. \quad (44)$$

where the constraint (43) follows from (5) and (7).

Also, to solve (P2) by convex optimization techniques, we express the following two lemmas.

Lemma 4.3: The throughput function of HGN i , $\forall i \in \{1, 2, \dots, K - \hat{K}\}$, given by $R_i^{hap}(\tau_{i,0})$ is a concave function of the nonnegative vector $\boldsymbol{\tau} = [\tau_{0,0}, \tau_{1,0}, \dots, \tau_{K-\hat{K},0}]^T$.

Proof: Please refer to Appendix D.

Lemma 4.4: The optimal time allocation $\boldsymbol{\tau}^*$ of (P2) has to satisfy the constraint in (43) with equality, i.e., $\sum_{i=1}^{K-\hat{K}} \tau_{i,0} = 1 - \tau_f - \tau_0^*$.

Proof: Please refer to Appendix E.

From Lemma 4.3, the objective of (P2) is a concave over $\boldsymbol{\tau}$ and also all the constraints of (P2) are affine from Lemma 4.4. Thus, Lagrangian duality is used to solve the (P2) with (43). The Lagrangian of (P2) can be formulated as

$$\mathcal{L}(\boldsymbol{\tau}, \lambda) = \sum_{j=1}^{K-\hat{K}} R_j^{hap}(\tau_{j,0}) - \lambda \left(\sum_{i=1}^{K-\hat{K}} \tau_{i,0} + \tau_0^* + \tau_f - 1 \right), \quad (45)$$

where $\lambda \geq 0$ denotes the Lagrange multipliers related to the constraint given in (43). The dual function of (P2) can be expressed as

$$\mathcal{G}(\lambda) = \max_{\boldsymbol{\tau} \in \mathcal{D}} \mathcal{L}(\boldsymbol{\tau}, \lambda), \quad (46)$$

where \mathcal{D} is the feasible set of $\boldsymbol{\tau}$ specified by (43) and (44). We obtain the optimal time allocation solution of (P2) as the following proposition

Proposition 4.2: The optimal time allocation of (P2) is

$$\tau_{i,0}^* = \frac{\bar{\varepsilon}_i}{\sum_{j=1}^{K-\hat{K}} \bar{\varepsilon}_j} (1 - \tau_0^* - \tau_f), \quad \forall i \in \{1, 2, \dots, K - \hat{K}\}. \quad (47)$$

where τ_0^* from (40).

Proof: Please refer to Appendix F.

IV. THE ANALYSIS OF THE WEIGHTED HARVEST-THEN-TRANSMIT PROTOCOL

In this section, we analyze the influence of the flight time, τ_f , in terms of the sum-throughput maximization, based on the UAV-enabled WPCN. The WHT protocol largely aims to overcome the *doubly-near-far* problem by using the UAV as a mobile H-AP to perform the weighted DL WET to LGNs. For the purpose of exposition, we simplify the network topology as nodes are located away from the H-AP at regular intervals in this section, and the first node is the nearest node and the last node is the farthest node from the H-AP. Note that regular intervals depend on the system of interest. Also, we assume that the number of nodes in the proposed network is 20, i.e., $K = 20$ and the number of HGNs and LGNs are same, i.e., $\hat{K} = 10$.

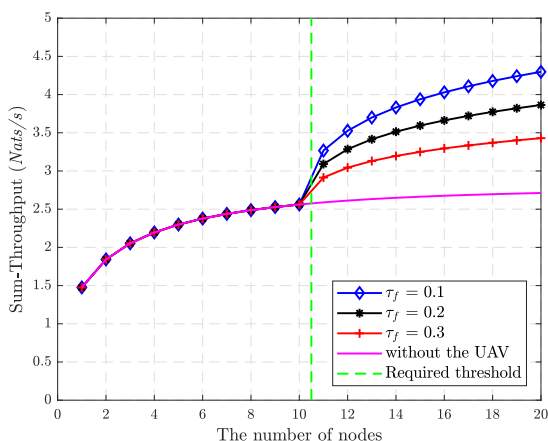


FIGURE 4. The sum-throughput according to the number of nodes in terms of the flight time.

Fig. 4 shows the sum-throughput according to the number of nodes where the sum-throughput means the total throughput of all nodes in the network. When τ_f is zero, i.e. without the UAV, LGNs can hardly transmit their information since they have trouble to harvest energy from the H-AP due to the *doubly-near-far* problem. On the other hand, when there is the UAV, i.e. $\tau_f > 0$, LGNs can harvest energy by the weighted DL WET from the UAV and transmit information to the UAV, using the harvested energy.

We compare the sum-throughput of all nodes when $\tau_f > 0$ as shown in Fig. 4. The sum-throughput of all nodes decreases as τ_f increases since the ratio of τ_f to a block time increases. From (7), the total weighted DL WET time, τ_0 , decreases as τ_f increases. Thus, the harvested energy at each LGN decreases. In addition, from (10), the total WIT time of LGNs, $\sum_{i=1}^{\hat{K}} \tau_i, \forall i \in \{1, 2, \dots, \hat{K}\}$, decreases as τ_f increases. Consequently, from (5), (7), and (10), the constraint of (P1) in (34) can be reformulated as

$$\tau_0 + \sum_{i=1}^{\hat{K}} \tau_i \leq 1 - 2\tau_f, \quad \forall i \in \{1, 2, \dots, \hat{K}\}. \quad (48)$$

Moreover, the energy causality constraint of the UAV in (17) limits the amount of the energy for the weighted DL WET, where Q_{flight} increases as τ_f increases.

V. NUMERICAL RESULTS

In this section, we present some numerical results to evaluate the performance of the proposed WHT protocol in the UAV-enabled WPCN. The harvest-then-transmit (HTT) protocol proposed in [13] is used as the reference protocol for the comparison. In the evaluation, we assume that the energy harvesting efficiency is 1 for all nodes, i.e., $\xi_i = 1, \forall i \in \{1, 2, \dots, K\}$. The noise power at the UAV, σ^2 , and at the H-AP, $\hat{\sigma}^2$, are assumed to be 1, respectively. Also, we assume that the transmit power at the H-AP for the DL WET, P_H , is 10 dB. In addition, we assume that *i.i.d.* Rayleigh fading for all channels and the channel power gains in the network are exponentially distributed. A channel power gain of each node is dependent on the regular interval, since a channel power gain is inversely proportional to the square of the distance in (1), (3), and the distance from the H-AP can be calculated by multiplying node index and regular interval. Finally, we assume UAV flies at a fixed altitude.

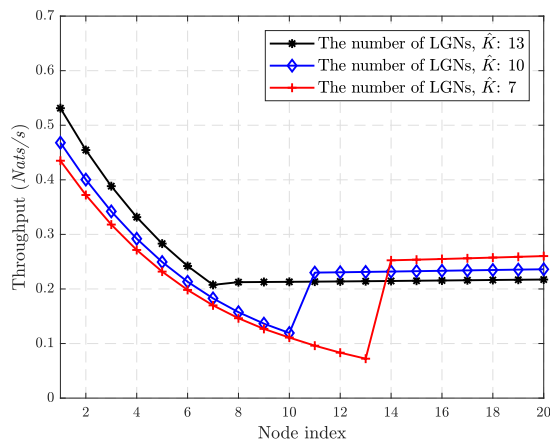


FIGURE 5. The throughput of each node according to the number of LGNs among nodes.

Fig. 5 shows the effect of the required threshold to the throughput of each node in the proposed WHT protocol. We assume that there are 20 nodes in the network, i.e., $K = 20$. The number of LGNs is defined by the required threshold in the system of interest, and the amount of harvested energy from the UAV at each LGN is dependent on the number of LGNs. In other words, the amount of harvested energy at each LGN increases with decreasing the number of LGNs since the total energy for the weighted DL WET at the UAV is limited. Therefore, the throughput of each LGN also increases according to decreasing the number of LGNs. On the other hand, the ratio of the number of HGNs and LGNs affects to the throughput balance among nodes in the network. When there are 13 HGNs, i.e., $\hat{K} = 7$, we can see that the minimum throughput among HGNs is terribly low compared to the throughput of LGNs. When there are 10 HGNs, i.e., $\hat{K} = 10$, the throughput gap between the minimum throughput among HGNs and LGNs is reduced compared to the previous case. Finally, when there are seven HGNs, i.e., $\hat{K} = 13$, the minimum throughput among HGNs and

the LGNs is almost same. Consequently, the proposed WHT protocol can improve the fairness in terms of throughput among nodes, or improve the communication performance of the LGNs rather than the HGNs by adjusting required threshold.

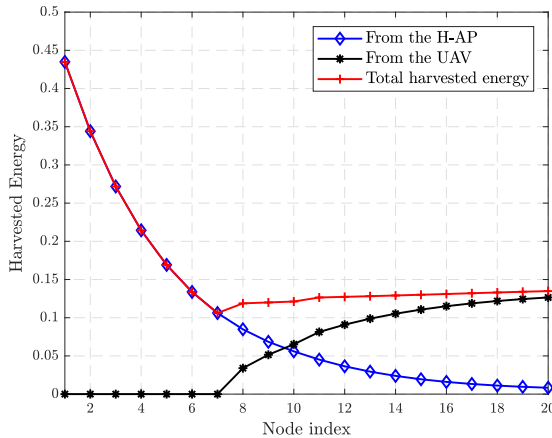


FIGURE 6. The harvested energy of each node according to the node index.

Fig. 6 shows the amount of harvested energy of each node when adopting the WHT protocol. We assume that there are 20 nodes in the network, i.e., $K = 20$. We also assume that the number of HGNs and LGNs are 7 and 13, respectively, since the nodes have the best fairness condition in that case in terms of throughput, as we can see in fig. 5. All nodes harvest energy from the H-AP, where the amount of the harvested energy decreases exponentially according to decreasing of the channel power gain to the H-AP. On the other hand, we can see that LGNs harvest additional energy from the UAV, and the amount of energy harvested from the UAV is inversely proportional to the channel power gain between the H-AP and each LGN in (16), i.e., far-apart LGN receives more energy from the UAV than near-apart LGN. Therefore, total harvested energy at each LGN is almost same each other. For the reason, each LGN transmits information to the UAV with almost uniform throughput, as shown in Fig. 5.

Fig. 7 shows the throughput of each node at regular decreasing intervals of channel gain when adopting the proposed WHT protocol and the HTT protocol, respectively. We assume that there are 20 nodes in the network, i.e., $K = 20$. We also assume that the number of HGNs and LGNs are 7 and 13, respectively, i.e., $\hat{K} = 13$. It means that the node 8 to node 20 have lower channel power gain to the H-AP than the required threshold in the system. In Fig. 7, the throughput decreases with increasing the regular decreasing intervals of channel gain in the both protocol. However, the throughput of each node in the WHT protocol is higher than the HTT protocol. Especially, we can see that LGNs perform UL WITs with greatly high throughput in the WHT protocol compared to the HTT protocol. This is because LGNs harvest additional energy from the UAV and transmit information directly to the UAV with better channel power gain.

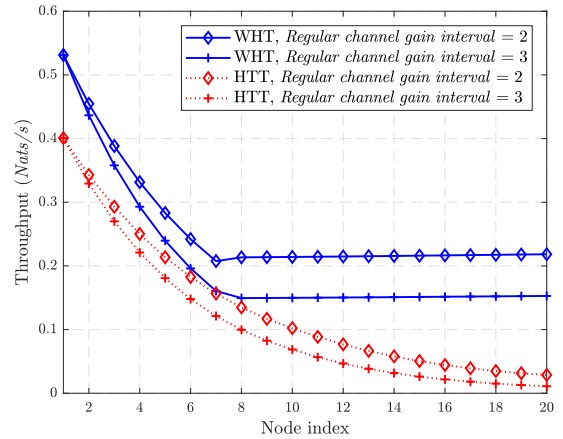


FIGURE 7. The throughput of each node according to the node index.

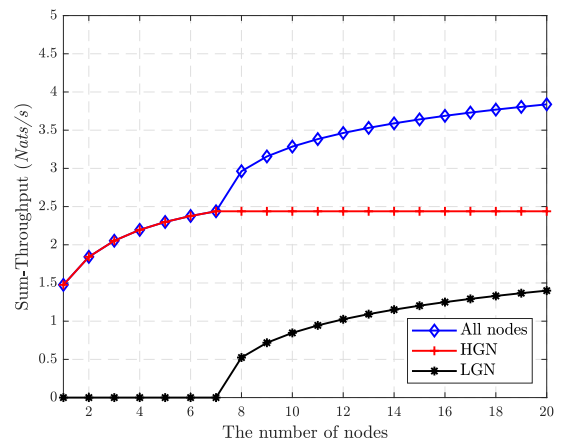


FIGURE 8. The sum-throughput of HGN and LGN according to the number of nodes.

Fig. 8 shows the sum-throughput according to the number of nodes in the proposed UAV-enabled WPCN when adopting the WHT protocol. We assume that the maximum number of nodes in the network is 20, i.e., $1 \leq K \leq 20$. In addition, we assume that all nodes are HGNs if the number of nodes is less than or equal to 7, thus the maximum number of HGNs can be 7, i.e., $1 \leq K - \hat{K} \leq 10$. When all existing nodes are the HGN, the sum-throughput of HGNs increases with increasing the number of nodes in the network. When the number of nodes exceeds the maximum number of HGN, i.e., the number of nodes is greater than or equal to 13, the sum-throughput of LGNs begins to increase with increasing the number of the nodes due to the additional energy transfer by the UAV. Consequently, the sum-throughput of all nodes increases with increasing the number of nodes, regardless of the channel power gain between the H-AP and each node.

VI. CONCLUSION

In this paper, we investigate the sum-throughput maximization problem in the UAV-enabled WPCN, where the UAV is employed as a mobile H-AP to tackle the doubly-near-far problem. The UAV performs the weighted DL WET to

encountering LGNs in the forward flight phase and then receives information from the LGNs in the return flight phase, based on the newly proposed *weighted harvest-then-transmit* protocol. Under these conditions, we first optimize the time allocation for the LGNs in a block time, considering the channel power gain and the flight time. The duration time of the DL and UL period for LGNs is determined by optimizing the weighted DL WET of the UAV. Given the optimal duration times, we also maximize the sum-throughput of all HGNs. The numerical results show that the proposed UAV-enabled WPCN supports improved communication in terms of throughput and fairness than the conventional WPCNs.

There are some future works to improve the proposed system model. More exquisite energy consumption model according to various flight trajectories for the UAV can be valuable for the feasibility of UAV-enabled WPCN. Additionally, we will expand the proposed model to employ channel fading model instead of quasi-static flat-fading and consider more sophisticated path-loss model rather than free-space in order to realize UAV-enabled WPCN.

APPENDIX A PROOF OF LEMMA 4.1

We denote the Hessian of $R_i^{uav}(\tau_i)$ by \mathbf{H}_i in order to show $R_i^{uav}(\tau_i)$ is a concave function of τ_i , $\forall i \in \{1, 2, \dots, \hat{K}\}$, since a function is concave if its Hessian is negative semidefinite according to [36]. Thus, we demonstrate that \mathbf{H}_i is negative semidefinite for any given real vector $\mathbf{v} = [v_0, \dots, v_K]^T$, which is given by

$$\mathbf{v}^T \mathbf{H}_i \mathbf{v} \leq 0, \quad (49)$$

where the inequality follows from the fact that $\tau_i \geq 0$. Therefore, $R_i^{uav}(\tau_i)$, $\forall i \in \{1, 2, \dots, \hat{K}\}$, is a concave function of $\tau = [\tau_0, \dots, \tau_{K-\hat{K}}]^T$, since \mathbf{H}_i is negative semidefinite.

This completes the proof of Lemma 4.1.

APPENDIX B PROOF OF LEMMA 4.2

This can be proved by contradiction. Suppose $\tau' = [\tau'_0, \dots, \tau'_{\hat{K}}]^T$ is an optimal solution of (P1), and it satisfies that $\sum_{i=0}^{\hat{K}} \tau_i < 1 - 2\tau_f$. It follows that $\tau'_0 < 1 - 2\tau_f - \sum_{i=1}^{\hat{K}} \tau_i$. The objective function given in (33) is a monotonic increasing function with respect to τ_0 . Thus, the value of (33) under the vector $[1 - 2\tau_f - \sum_{i=1}^{\hat{K}} \tau_i, \tau'_1, \dots, \tau'_{\hat{K}}]^T$ is larger than that under τ' . This contradicts with our presumption. Thus, the optimal τ^* must satisfy $\sum_{i=0}^{\hat{K}} \tau_i^* = 1 - 2\tau_f$.

This completes the proof of Lemma 4.2.

APPENDIX C PROOF OF PROPOSITION 4.1

The Lagrangian of (P1) is

$$\mathcal{L}(\tau, \lambda) = \sum_{i=1}^{\hat{K}} R_i^{uav}(\tau_i) - \lambda \left(\sum_{i=0}^{\hat{K}} \tau_i + 2\tau_f - 1 \right), \quad (50)$$

where λ is the non-negative Lagrangian dual variable related to constraint given in (34).

The dual function of (P1) is given by

$$\mathcal{G}(\lambda) = \max_{\tau \in \mathcal{D}} \mathcal{L}(\tau, \lambda), \quad (51)$$

where \mathcal{D} is the feasible set of τ specified by the constraints (34) and (35). It is observed that there exists an $\tau \in \mathcal{D}$ with all strict positive elements satisfying $\sum_{i=0}^{\hat{K}} \tau_i \leq 1 - 2\tau_f$. Thus, strong duality holds for the problem since the Slater's condition [36] is satisfied. Therefore, Karush-Kuhn-Tucker (KKT) conditions are sufficient to solve (P1), which are given by

$$Q_{wdl} \geq 0, \quad v_{uav} \geq 0, \quad (52)$$

$$\lambda^* \geq 0, \quad \tau_i \geq 0, \quad \forall i \in \{0, 1, \dots, \hat{K}\}, \quad (53)$$

$$\sum_{i=0}^{\hat{K}} \tau_i^* \leq 1 - 2\tau_f, \quad (54)$$

$$\lambda^* \left(\sum_{i=0}^{\hat{K}} \tau_i^* + 2\tau_f - 1 \right) = 0, \quad (55)$$

$$\frac{\partial \mathcal{L}(\tau, \lambda^*)}{\partial \tau_i} \Big|_{\tau_i = \tau_i^*} = 0, \quad \forall i \in \{0, 1, \dots, \hat{K}\}, \quad (56)$$

where τ_i^* and λ^* denote the optimal primal and dual solutions of (P1), respectively. Then, from (56), it follows that

$$\sum_{i=1}^{\hat{K}} \frac{\hat{\varepsilon}_i}{1 + \varepsilon_i \frac{1}{\tau_i^*} + \hat{\varepsilon}_i \frac{\tau_0^*}{\tau_i^*}} = \lambda^*, \quad (57)$$

$$\mathcal{B}_i \left(\varepsilon_i \frac{1}{\tau_i^*} + \hat{\varepsilon}_i \frac{\tau_0^*}{\tau_i^*} \right) = \lambda^*, \quad \forall i \in \{1, 2, \dots, \hat{K}\}, \quad (58)$$

where $\mathcal{B}_i(x)$ is defined as

$$\mathcal{B}_i(x) \triangleq \ln(1+x) - \frac{x}{1+x}, \quad \forall i \in \{1, 2, \dots, \hat{K}\}. \quad (59)$$

Given $1 \leq i, j \leq \hat{K}$, from (57) we have

$$\mathcal{B}_i \left(\varepsilon_i \frac{1}{\tau_i^*} + \hat{\varepsilon}_i \frac{\tau_0^*}{\tau_i^*} \right) = \mathcal{B}_j \left(\varepsilon_j \frac{1}{\tau_j^*} + \hat{\varepsilon}_j \frac{\tau_0^*}{\tau_j^*} \right), \quad i \neq j. \quad (60)$$

Since $\mathcal{B}_i(x)$ is a monotonically increasing function of $x \geq 0$, i.e., $\frac{d\mathcal{B}_i(x)}{dx} \geq 0$ for $x \geq 0$, equality in (60) holds if and only if $\varepsilon_i \frac{1}{\tau_i^*} + \hat{\varepsilon}_i \frac{\tau_0^*}{\tau_i^*} = \varepsilon_j \frac{1}{\tau_j^*} + \hat{\varepsilon}_j \frac{\tau_0^*}{\tau_j^*}$, $1 \leq i, j \leq \hat{K}$, i.e.,

$$\frac{\varepsilon_1}{\tau_1^*} = \frac{\varepsilon_2}{\tau_2^*} = \dots = \frac{\varepsilon_{\hat{K}}}{\tau_{\hat{K}}^*} = A. \quad (61)$$

$$\frac{\hat{\varepsilon}_1}{\tau_1^*} = \frac{\hat{\varepsilon}_2}{\tau_2^*} = \dots = \frac{\hat{\varepsilon}_{\hat{K}}}{\tau_{\hat{K}}^*} = B. \quad (62)$$

From (54) and (62), τ_i^* can be expressed as

$$\tau_i^* = \frac{\hat{\varepsilon}_i}{\sum_{j=1}^{\hat{K}} \hat{\varepsilon}_j} (1 - \tau_0^* - 2\tau_f). \quad (63)$$

In addition, it follows from (56), (62), and (63) that

$$\begin{aligned} \ln(1 + B(\frac{\varepsilon_{\hat{K}}}{\hat{\varepsilon}_{\hat{K}}} + \tau_0^*)) - \frac{B(\frac{\varepsilon_{\hat{K}}}{\hat{\varepsilon}_{\hat{K}}} + \tau_0^*)}{1 + B(\frac{\varepsilon_{\hat{K}}}{\hat{\varepsilon}_{\hat{K}}} + \tau_0^*)} \\ = \frac{\sum_{i=1}^{\hat{K}} \hat{\varepsilon}_i}{1 + B(\frac{\varepsilon_{\hat{K}}}{\hat{\varepsilon}_{\hat{K}}} + \tau_0^*)}, \quad \forall i \in \{1, 2, \dots, \hat{K}\}, \end{aligned} \quad (64)$$

where $A = \frac{\varepsilon_{\hat{K}}}{\hat{\varepsilon}_{\hat{K}}} B$. Since $B = \frac{\sum_{i=1}^{\hat{K}} \hat{\varepsilon}_i}{1 - \tau_0^* - 2\tau_f}$ from (63), we can modify (64) as

$$\ln z - \frac{z - 1}{z} = \frac{C}{z}, \quad (65)$$

where $C = \sum_{i=1}^{\hat{K}} \hat{\varepsilon}_i$ and $z = 1 + \frac{\sum_{i=1}^{\hat{K}} \hat{\varepsilon}_i}{1 - \tau_0^* - 2\tau_f} (\frac{\varepsilon_{\hat{K}}}{\hat{\varepsilon}_{\hat{K}}} + \tau_0^*)$. It is observed that $z > 1$ if $C > 0$ and $0 < \tau_0^* < 1$. From (65), we have

$$\frac{\partial}{\partial z} f(z) = \ln z, \quad (66)$$

$$\frac{\partial^2}{\partial z^2} f(z) = \frac{1}{z}, \quad (67)$$

where $f(z) = z \ln z - z + 1$. Thus, $f(z)$ is a convex function over $z \geq 0$. Therefore, since $f(z) = C$ has a unique solution $z^* > 1$, given $C > 0$, the optimal time allocation to τ_0^* is given by

$$\tau_0^* = \frac{z^*(1 - \tau_f) - 1 + 2\tau_f - C \frac{\varepsilon_{\hat{K}}}{\hat{\varepsilon}_{\hat{K}}}}{C + z^* - 1} \quad (68)$$

In addition, from (63) and (68), the optimal time allocation to τ_i^* is given by

$$\tau_i^* = \frac{\hat{\varepsilon}_i}{C} \left(\frac{C(1 - \frac{\varepsilon_{\hat{K}}}{\hat{\varepsilon}_{\hat{K}}}) - z^* + 4\tau_f}{C + z^* - 1} - 2\tau_f \right). \quad (69)$$

This completes the proof of Proposition 4.1.

APPENDIX D

PROOF OF LEMMA 4.3

Given in (28), $R_i^{hap}, \forall i \in \{1, 2, \dots, K - \hat{K}\}$, is a concave function since $R_i^{hap}(\tau_{i,0})$ is a composition of a concave function $\hat{R}_i(x) = \ln(1 + x)$ and $\bar{R}_i(\tau) = \frac{1}{\tau}$, i.e., $R_i^{hap}(\tau_{i,0}) = \hat{R}_i(\bar{R}_i(\tau))$.

This completes the proof of Lemma 4.3.

APPENDIX E

PROOF OF LEMMA 4.4

We may note that the proof of Lemma 4.4 is essentially equal to Lemma 4.2.

Please refer to Appendix B.

APPENDIX F

PROOF OF PROPOSITION 4.2

The Lagrangian of (P2) is

$$\mathcal{L}(\boldsymbol{\tau}, \lambda) = \sum_{j=1}^{K-\hat{K}} R_j^{hap}(\tau_j, 0) - \lambda \left(\sum_{i=1}^{K-\hat{K}} \tau_{i,0} + \tau_0^* + \tau_f - 1 \right), \quad (70)$$

where $\lambda \geq 0$ denotes the Lagrange multipliers related to the constraint given in (43). The dual function of (P2) is given by

$$\mathcal{G}(\lambda) = \max_{\boldsymbol{\tau} \in \mathcal{D}} \mathcal{L}(\boldsymbol{\tau}, \lambda), \quad (71)$$

where \mathcal{D} is the feasible set of $\boldsymbol{\tau}$ specified by (43) and (44).

There exists an $\boldsymbol{\tau} \in \mathcal{D}$ with all strict positive elements satisfying $\sum_{j=1}^{K-\hat{K}} \tau_{j,0} \leq 1 - \tau_0^* - \tau_f$. Thus, strong duality holds for the problem since the Slater's condition [36] is satisfied. Consequently, KKT conditions are sufficient to solve (P2), which are given by

$$\lambda^* \geq 0, \quad \tau_{j,0} \geq 0, \quad \forall j \in \{0, 1, \dots, K - \hat{K}\}, \quad (72)$$

$$\sum_{j=1}^{K-\hat{K}} \tau_{j,0}^* \leq 1 - \tau_0^* - \tau_f, \quad (73)$$

$$\lambda^* \left(\sum_{j=1}^{K-\hat{K}} \tau_{j,0}^* + \tau_0^* + \tau_f - 1 \right) = 0, \quad (74)$$

$$\left. \frac{\partial \mathcal{L}(\boldsymbol{\tau}, \lambda^*)}{\partial \tau_{j,0}} \right|_{\tau_{j,0} = \tau_{j,0}^*} = 0, \quad \forall j \in \{1, 2, \dots, K - \hat{K}\}, \quad (75)$$

where $\boldsymbol{\tau} = [\tau_{0,0}, \tau_{1,0}, \dots, \tau_{\hat{K},0}]^T$. $\tau_{j,0}^*$ and λ^* denote the optimal primal and dual solutions of (P2), respectively. From (75), it follows that

$$\ln(1 + \bar{\varepsilon}_j \frac{1}{\tau_{j,0}^*}) - \frac{\frac{1}{\tau_{j,0}^*}}{1 + \frac{1}{\tau_{j,0}^*}} = \lambda^*, \quad \forall j \in \{1, 2, \dots, K - \hat{K}\}. \quad (76)$$

From (72), we consider the case of $\lambda^* > 0$, which corresponds to $\sum_{j=1}^{K-\hat{K}} \tau_{j,0}^* + \tau_0^* + \tau_f = 1$ from (74). Given $1 \leq i, j \leq K - \hat{K}$ in (76), we have equal result at $i \neq j$, since (76) is a monotonically increasing function as (60), i.e., $\tau_{j,0} = \frac{\bar{\varepsilon}_i}{\bar{\varepsilon}_j} \tau_{i,0}$. Hence, the optimal time allocation to $\tau_{i,0}^*$ is

$$\tau_{i,0}^* = \frac{\bar{\varepsilon}_i}{\sum_{j=1}^{K-\hat{K}} \bar{\varepsilon}_j} (1 - \tau_0^* - \tau_f), \quad \forall i \in \{1, 2, \dots, K - \hat{K}\}. \quad (77)$$

This completes the proof of Proposition 4.2.

ACKNOWLEDGMENT

(Sungryoung Cho and Kyungrak Lee contributed equally to this work.)

REFERENCES

- [1] X. Lu, P. Wang, D. Niyato, D. I. Kim, and Z. Han, "Wireless charging technologies: Fundamentals, standards, and network applications," *IEEE Commun. Surveys Tuts.*, vol. 18, no. 2, pp. 1413–1452, 2nd Quart., 2015.
- [2] Y. Zeng, B. Clerckx, and R. Zhang, "Communications and signals design for wireless power transmission," *IEEE Trans. Commun.*, vol. 65, no. 5, pp. 2264–2290, May 2017.
- [3] L. R. Varshney, "Transporting information and energy simultaneously," in *Proc. IEEE ISIT*, Toronto, ON, Canada, Jul. 2008, pp. 1612–1616.
- [4] S. Bi, C. K. Ho, and R. Zhang, "Wireless powered communication: Opportunities and challenges," *IEEE Commun. Mag.*, vol. 53, no. 4, pp. 117–125, Apr. 2015.
- [5] S. Bi, Y. Zeng, and R. Zhang, "Wireless powered communication networks: An overview," *IEEE Wireless Commun.*, vol. 23, no. 2, pp. 10–18, Apr. 2016.

- [6] K. W. Choi, L. Ginting, P. A. Rosyady, A. A. Aziz, and D. I. Kim, "Wireless-powered sensor networks: How to realize," *IEEE Trans. Wireless Commun.*, vol. 16, no. 1, pp. 221–234, Jan. 2017.
- [7] D.-W. Seo, J.-H. Lee, and H. Lee, "Method for adjusting single matching network for high-power transfer efficiency of wireless power transfer system," *ETRI J.*, vol. 38, no. 5, pp. 962–971, Oct. 2016.
- [8] X. Zhou, R. Zhang, and C. K. Ho, "Wireless information and power transfer: Architecture design and rate-energy tradeoff," *IEEE Trans. Commun.*, vol. 61, no. 11, pp. 4754–4767, Nov. 2013.
- [9] L. Liu, R. Zhang, and K.-C. Chua, "Wireless information and power transfer: A dynamic power splitting approach," *IEEE Trans. Commun.*, vol. 61, no. 9, pp. 3990–4001, Sep. 2013.
- [10] R. Zhang and C. K. Ho, "MIMO broadcasting for simultaneous wireless information and power transfer," *IEEE Trans. Wireless Commun.*, vol. 12, no. 5, pp. 1989–2001, May 2013.
- [11] K. Huang and E. Larsson, "Simultaneous information and power transfer for broadband wireless systems," *IEEE Trans. Signal Process.*, vol. 61, no. 23, pp. 5972–5986, Dec. 2013.
- [12] X. Zhou, R. Zhang, and C. K. Ho, "Wireless information and power transfer in multiuser OFDM systems," *IEEE Trans. Wireless Commun.*, vol. 13, no. 4, pp. 2282–2294, Apr. 2014.
- [13] H. Ju and R. Zhang, "Throughput maximization in wireless powered communication networks," *IEEE Trans. Wireless Commun.*, vol. 13, no. 1, pp. 418–428, Jan. 2014.
- [14] H. Ju and R. Zhang, "Optimal resource allocation in full-duplex wireless-powered communication network," *IEEE Trans. Commun.*, vol. 62, no. 10, pp. 3528–3540, Oct. 2014.
- [15] X. Kang, C. K. Ho, and S. Sun, "Full-duplex wireless-powered communication network with energy causality," *IEEE Trans. Wireless Commun.*, vol. 14, no. 10, pp. 5539–5551, Oct. 2015.
- [16] H. Ju, Y. Lee, and T.-J. Kim, "Full-duplex operations in wireless powered communication networks," *ETRI J.*, vol. 39, no. 6, pp. 794–802, Dec. 2017.
- [17] J. I. Choi, M. Jain, K. Srinivasan, P. Levis, and S. Katti, "Achieving single channel, full duplex wireless communication," in *Proc. 16th Annu. Int. Conf. Mobile Comput. Netw.*, New York, NY, USA, 2010, pp. 1–12.
- [18] K. Lee, S. Cho, J. Lee, and I. Joe, "Harvest-then-transceive: Throughput maximization in full-duplex wireless-powered communication networks," *IEICE Trans. Commun.*, vol. E101.B, no. 4, pp. 1128–1141, Apr. 2018.
- [19] S. Cho, K. Lee, B. J. Kang, and I. Joe, "A hybrid MAC protocol for optimal channel allocation in large-scale wireless powered communication networks," *EURASIP J. Wireless Commun. Netw.*, vol. 2018, no. 1, pp. 1–13, Dec. 2018. [Online]. Available: <https://citation-needed.springer.com/v2/references/10.1186/s13638-017-1012-2?format=bibtex&flavour=citation>
- [20] H. Tabassum, E. Hossain, A. Ogundipe, and D. I. Kim, "Wireless-powered cellular networks: Key challenges and solution techniques," *IEEE Commun. Mag.*, vol. 53, no. 6, pp. 63–71, Jun. 2015.
- [21] H. Chen, Y. Li, J. L. Rebelatto, B. F. Uchôa-Filho, and B. Vucetic, "Harvest-then-cooperate: Wireless-powered cooperative communications," *IEEE Trans. Signal Process.*, vol. 63, no. 7, pp. 1700–1711, Apr. 2015.
- [22] S. Bi and R. Zhang, "Placement optimization of energy and information access points in wireless powered communication networks," *IEEE Trans. Wireless Commun.*, vol. 15, no. 3, pp. 2351–2364, Mar. 2016.
- [23] T. S. Rappaport, *Wireless Communications: Principles and Practice*, 2nd ed. Englewood Cliffs, NJ, USA: Prentice-Hall, 2001.
- [24] Q. Yao, A. Huang, H. Shan, T. Q. S. Quek, and W. Wang, "Delay-aware wireless powered communication networks—Energy balancing and optimization," *IEEE Trans. Wireless Commun.*, vol. 15, no. 8, pp. 5272–5286, Aug. 2016.
- [25] J. Zhang, Y. Zeng, and R. Zhang, "Spectrum and energy efficiency maximization in UAV-enabled mobile relaying," in *Proc. IEEE ICC*, Paris, France, May 2017, pp. 1–6.
- [26] C. Zhan, Y. Zeng, and R. Zhang, "Energy-efficient data collection in UAV enabled wireless sensor network," *IEEE Wireless Commun. Lett.*, vol. 7, no. 3, pp. 328–331, Jun. 2018.
- [27] Y. Zeng, J. Lyu, and R. Zhang, "Cellular-connected UAV: Potentials, challenges and promising technologies," *IEEE Wireless Commun.*, to be published. [Online]. Available: <https://arxiv.org/abs/1804.02217>
- [28] J. Xu, Y. Zeng, and R. Zhang, "UAV-enabled wireless power transfer: Trajectory design and energy region characterization," in *Proc. IEEE Globecom Workshops (GC Wkshps)*, Singapore, Dec. 2017, pp. 1–7.
- [29] J. Xu, Y. Zeng, and R. Zhang, "UAV-enabled multiuser wireless power transfer: Trajectory design and energy optimization," in *Proc. 23rd Asia-Pacific Conf. Commun. (APCC)*, Perth, WA, Australia, Dec. 2017, pp. 1–6.
- [30] L. Xie, J. Xu, and R. Zhang, "Throughput maximization for UAV-enabled wireless powered communication networks," *IEEE Veh. Technol. Soc.*, to be published. [Online]. Available: <https://arxiv.org/abs/1801.04545>
- [31] A. Rotnitzky and N. P. Jewell, "Hypothesis testing of regression parameters in semiparametric generalized linear models for cluster correlated data," *Biometrika*, vol. 77, no. 3, pp. 485–497, 1990.
- [32] Y.-H. Ko, K.-J. Kim, and C.-H. Jun, "A new loss function-based method for multiresponse optimization," *J. Qual. Technol.*, vol. 37, no. 1, pp. 50–59, 2005.
- [33] X. Wang, S. Sha, J. He, L. Guo, and M. Lu, "Wireless power delivery to low-power mobile devices based on retro-reflective beamforming," *IEEE Antennas Wireless Propag. Lett.*, vol. 13, pp. 919–922, 2014.
- [34] T. Zhang, "Solving large scale linear prediction problems using stochastic gradient descent algorithms," in *Proc. 21st Int. Conf. Mach. Learn. (ICML)*, Banff, AB, Canada, 2004, p. 116.
- [35] Q. Yao, A. Huang, H. Shan, T. Q. S. Quek, and W. Wang, "Adaptive harvest-then-cooperate: Delay-aware wireless powered communication networks," in *Proc. IEEE 17th Int. Workshop Signal Process. Adv. Wireless Commun. (SPAWC)*, Edinburgh, U.K., Jul. 2016, pp. 1–5.
- [36] S. Boyd and L. Vandenberghe, *Convex Optimization*. Cambridge, U.K.: Cambridge Univ. Press, 2004.



powered communication sensor network.

SUNGRYUNG CHO received the B.S. degree in electrical engineering and computer science from Kookmin University, Seoul, South Korea, in 2012. He is currently pursuing the Ph.D. degree in computer and software with Hanyang University, Seoul.

Since 2008, he has been a Senior Researcher with IMPEC Enterprise, Uiwang, South Korea. His research interests include convex optimization, probability theory, energy harvesting, wireless-

powered communication networks, unmanned aerial vehicle, and wireless



wireless sensor networks, Internet of Things, zigbee, and wireless powered communication networks.

KYUNGRAK LEE received the B.S., M.S., and Ph.D. degrees in electronics and computer engineering from Hanyang University, Seoul, South Korea, in 2008, 2010, and 2018, respectively.

He is currently a Senior Researcher with the Electronics and Telecommunications Research Institute, Daejeon, South Korea. His research interests include unmanned vehicle systems, deep space communication, delay tolerant network, wireless sensor networks, Internet of Things, zigbee, and wireless powered communication networks.



BOOJOONG KANG received the B.S., M.S., and Ph.D. degrees in electronics and computer engineering from Hanyang University, Seoul, South Korea, in 2007, 2009, and 2013, respectively.

He is currently a Research Fellow with the Centre for Secure Information Technologies, Queen's University Belfast, U.K. His research interests include cyber security in various networked systems and computer networks.



KWANGMIN KOO received the B.S. degree in computer and software from Sangmyung University, Cheonan, South Korea, in 2016. He is currently pursuing the M.S. degree with the Department of Computer and Software, Hanyang University, Seoul.

His current research interests include computer networks, deep learning, big data processing, delay tolerant network, and blockchain.



INWHEE JOE received the B.S. and M.S. degrees in electronics engineering from Hanyang University, Seoul, South Korea, and the Ph.D. degree in electrical and computer engineering from the Georgia Institute of Technology, Atlanta, GA, USA, in 1998.

Since 2002, he has been a Faculty Member with the Division of Computer Science and Engineering, Hanyang University, Seoul. His current research interests include Internet of Things, cellular systems, wireless power communication networks, embedded systems, network security, machine learning, and performance evaluation.

• • •